

Highly directional pressure sensing using the phase gradient

Joseph S. Lawrence, Kent L. Gee, Tracianne B. Neilsen, and Scott D. Sommerfeldt

Citation: [The Journal of the Acoustical Society of America](#) **144**, EL346 (2018); doi: 10.1121/1.5065401

View online: <https://doi.org/10.1121/1.5065401>

View Table of Contents: <http://asa.scitation.org/toc/jas/144/4>

Published by the [Acoustical Society of America](#)

Articles you may be interested in

[Three-microphone probe bias errors for acoustic intensity and specific acoustic impedance](#)

[The Journal of the Acoustical Society of America](#) **143**, EL81 (2018); 10.1121/1.5022688

Highly directional pressure sensing using the phase gradient

Joseph S. Lawrence, Kent L. Gee, Tracianne B. Neilsen,
and Scott D. Sommerfeldt

Department of Physics and Astronomy, Brigham Young University, Provo,
Utah 84602, USA

joseph-lawrence@hotmail.com, kentgee@byu.edu, tbn@byu.edu,
scott_sommerfeldt@byu.edu

Abstract: Many methods of two-microphone directional sensing have limited bandwidth. For active intensity, finite-difference error can be removed by using the phase and amplitude gradient estimator method. Using similar principles, a directional pressure sensor based on the phase gradient is developed that is accurate up to the spatial Nyquist frequency, and beyond if phase unwrapping is applied. A highly directional frequency-independent array response of arbitrary order can be achieved with two microphones. The method is compared against beamforming and traditional gradient sensing for single and multiple sources and is found to have improved localization capabilities and increased bandwidth.

© 2018 Acoustical Society of America
[CCC]

Date Received: June 19, 2018 **Date Accepted:** October 9, 2018

1. Introduction

Directional pressure sensors have a variety of uses, including direction finding, energy-based quantity estimation, and source discrimination. One common approach is pressure gradient sensing using a microphone array, such as in the case of a cardioid microphone.^{1–3} Pressure gradient sensors serve as a basis for intensity estimation, and can be extended to create higher-order sensors such as a particle velocity gradient sensor.^{4–7} Another approach is beamforming, using time (or phase) delays to steer a microphone array in arbitrary directions.^{8,9} Several more complicated methods of directional sensing exist.^{10–14}

Recently, the phase and amplitude gradient estimator (PAGE) method has been developed to increase estimation bandwidth for multi-microphone acoustic vector intensity estimation.¹⁵ Traditional intensity estimation bandwidth depends on the microphone spacing, with accuracy decreasing as the spatial Nyquist frequency is approached. The PAGE method relies on the phase gradient, allowing accuracy up to the spatial Nyquist frequency for propagating fields. For broadband sources and with sufficient coherence between the microphones,¹⁶ the phase gradient can be unwrapped,¹⁷ allowing the method to be accurate at frequencies much higher than the spatial Nyquist frequency.¹⁸ In this letter, we report a method similar to PAGE for directional pressure rather than intensity. The method utilizes the phase gradient to outperform traditional gradient sensors for frequency-dependent source localization using two microphones, showing improvements in both bandwidth and directionality.

2. Theory

As shown by Bastyr,⁴ the continuity equation can be used to estimate pressure using spatial derivatives of the particle velocity. This estimate can be combined with particle velocity to create a u - u intensity sensor, or used alone as a directional pressure sensor as done by de Bree and Wind.⁵ For a time-harmonic process with $e^{j\omega t}$ dependence, complex pressure relates to the divergence of the particle velocity as

$$p = \frac{j\rho_0 c^2}{\omega} \nabla \cdot \mathbf{u}, \quad (1)$$

where ρ_0 is the air density, c is the sound speed, ω is the angular frequency, \mathbf{u} is the particle velocity, and $j = \sqrt{-1}$. In Cartesian coordinates, the divergence in Eq. (1) is separated into three components, expressing the complex pressure as a summation,

$$p = \frac{j\rho_0 c^2}{\omega} \left[\frac{\partial u_x}{\partial x} + \frac{\partial u_y}{\partial y} + \frac{\partial u_z}{\partial z} \right]. \quad (2)$$

In the far field of a source, the three derivative terms in Eq. (2) each represent sound pressure corresponding with particle motion in a single direction. Pressure from a single direction can be evaluated with a one-dimensional array, used to estimate a single derivative from Eq. (2),

$$p_x = \frac{j\rho_0 c^2}{\omega} \frac{\partial u_x}{\partial x}, \quad (3)$$

where x is the direction along the array axis. This directional pressure quantity can be estimated using two particle velocity sensors and a finite difference. Alternatively, since particle velocity can be related to the pressure gradient through the time-harmonic Euler equation, the directional pressure in Eq. (3) can be obtained using three microphones in a line to estimate a second derivative of pressure. The directivity associated with these derivatives produces a $\cos^2\theta$ array response, where θ is the angle from the array axis to the source.

In estimating Eq. (3) using multiple sensors, finite-difference errors cause high-frequency inaccuracy, as the wavelength becomes small relative to the microphone separation.¹⁸ The PAGE method was developed to remove such errors in frequency-domain active intensity. By expressing pressure as an amplitude, P , and a phase, ϕ , Euler's equation for particle velocity takes a new form that relies on the unwrapped phase gradient. The particle velocity is estimated as

$$\mathbf{u} = \frac{e^{-j\phi}}{\rho_0 \omega} (P \nabla \phi + j \nabla P), \quad (4)$$

where P and $\nabla \phi$ at the acoustic center of the array are estimated using a finite-sum and a finite-difference, respectively. For a plane wave, P is constant in space and ϕ changes linearly in space, allowing the center estimates in Eq. (4) to be accurate up to the spatial Nyquist frequency.¹⁸ Additionally, the method can be accurate beyond the spatial Nyquist frequency for broadband sources when phase unwrapping can be properly applied.¹⁷ This is opposed to traditional intensity estimation which, due to errors in estimation of the complex pressure average and gradient, becomes less accurate as the spatial Nyquist frequency is approached.

The PAGE expression for particle velocity can be used in a directional pressure sensor, overcoming finite-sum and finite-difference error but restricting the method to the frequency domain. By substituting Eq. (4) into Eq. (3), the contribution to pressure in the direction of the array axis can be expressed in terms of the frequency-domain quantities P and ϕ as

$$p_x = \frac{1}{k^2} \left[P \left(\frac{\partial \phi}{\partial x} \right)^2 - \frac{\partial^2 P}{\partial x^2} + jP \frac{\partial^2 \phi}{\partial x^2} + 2j \frac{\partial P}{\partial x} \frac{\partial \phi}{\partial x} \right] e^{-j\phi}, \quad (5)$$

where $k = \omega/c$ is the acoustic wavenumber. Each of the phase derivatives in Eq. (5) can be estimated using the phase of transfer functions between microphones, removing finite-difference error and extending bandwidth up to the spatial Nyquist frequency, and even higher when the phase can be unwrapped.

To investigate the behavior of Eq. (5), each term can be evaluated in a monopole field. For a source at the origin, the monopole pressure field is $P = A/r = A/\sqrt{x^2 + y^2}$ and $\phi = kr = k\sqrt{x^2 + y^2}$, where A is amplitude, r is the distance between the acoustic center of the array and the source, and x and y are components of r , with x being the component of r along the array axis. Partial derivatives of P and ϕ in Eq. (5) are evaluated for the monopole field (for example, $\partial \phi / \partial x = kx/\sqrt{x^2 + y^2} = k \cos \theta$), resulting in the response

$$p_{x,\text{monopole}} = \frac{A}{k^2} \left[\frac{k^2}{r} \cos^2 \theta + \left(\frac{jk}{r^2} + \frac{1}{r^3} \right) (\sin^2 \theta - 2 \cos^2 \theta) \right] e^{-j\phi}. \quad (6)$$

This response is shown in Fig. 1(a) for several frequencies, for $r = 2.1$ m (7 ft). The first term in Eq. (5) results in a $\cos^2\theta$ response at all distances, represented by the first term in Eq. (6). The remainder of Eq. (6) results from the last three terms in Eq. (5), altering the response in the near field, with a $\sin^2\theta$ term creating a significant response when pointing perpendicular to the source ($\theta = 90^\circ$). Therefore, using components of the divergence as done by de Bree and Wind⁵ leads to ineffective direction finding in the near field.

In order to achieve a $\cos^2\theta$ response in both the near and the far field for direction finding, Eq. (5) can be modified to retain only the far-field term. This creates

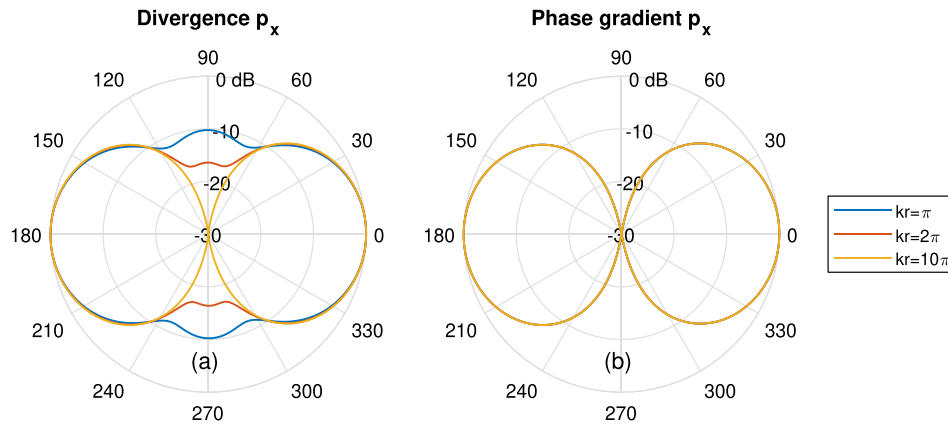


Fig. 1. (Color online) Theoretical response for (a) divergence-based [Eq. (5)] and (b) phase gradient-based [Eq. (7)] directional pressure components as a function of angle θ for several values of kr , where r is fixed to be 2.1 m (7 ft).

a directional pressure sensor based on the phase gradient, with an identical response to Eq. (5) at the far-field limit and improved direction finding in the near field. The sensor is expressed as

$$p_x = \frac{1}{k^2} \left(\frac{\partial \phi}{\partial x} \right)^2 P e^{-j\phi} \quad (7)$$

and is shown in Fig. 1(b) to have a response unaltered by distance to the source. Additionally, Eq. (7) contains no second derivatives, so p_x can be estimated using two microphones instead of three.

The phase gradient sensor in Eq. (7) represents a method for splitting the pressure into directional components, different from the particle velocity divergence components in Eq. (2) and valid at all distances from a monopole source. In a monopole field, the magnitude of the phase gradient is $|\nabla \phi| = k$, regardless of microphone separation or source distance. Therefore, p can be expressed as

$$p = \frac{1}{k^2} |\nabla \phi|^2 P e^{-j\phi} = \frac{1}{k^2} \left[\left(\frac{\partial \phi}{\partial x} \right)^2 + \left(\frac{\partial \phi}{\partial y} \right)^2 + \left(\frac{\partial \phi}{\partial z} \right)^2 \right] P e^{-j\phi}, \quad (8)$$

such that the complex pressure is expressed as a summation of three components in orthogonal directions. As opposed to divergence-based components in Eq. (2), Eq. (8) contains components of the phase gradient, which relate directly to the sound propagation. Since active intensity can also be expressed in terms of the phase gradient,¹⁵ a single directional pressure component has a maximum response in the same direction as a one-dimensional intensity estimate, but with a $\cos^2 \theta$ response as opposed to a $\cos \theta$ response, providing a smaller beam width and increased directivity.

An additional advantage of using phase gradient-based directional pressure is the possibility to achieve an arbitrary array response through modification of Eq. (7). Since the relative array response is simply a function of $(\partial \phi / \partial x) / k$, a modification of this directivity factor changes the response of the array. Several possibilities for improving array response are discussed in the remainder of this section.

A higher-order bidirectional sensor can be created to achieve an array response narrower than $\cos^2 \theta$. This is done by changing the power on the directivity factor in Eq. (7), raising it to an arbitrary power M , resulting in

$$p_{x,M} = \frac{1}{k^M} \left(\frac{\partial \phi}{\partial x} \right)^M P e^{-j\phi}, \quad (9)$$

which achieves a $\cos^M \theta$ array response with the use of only two microphones. Figure 2(a) shows the simulated response with different values of M , showing tighter beam widths up to $M = 8$. With real data, any noise in the transfer function phase is included in the factor raised to the power of M in Eq. (9), such that along the array axis the noise is amplified at least linearly with M . Therefore, depending on the amount of noise in the phase, a power of M should be chosen that tightens the beam width without overly corrupting the signal with amplified noise.

In many cases, it may be beneficial to have an array response that is unidirectional instead of bidirectional, such that the array is sensitive in one direction instead

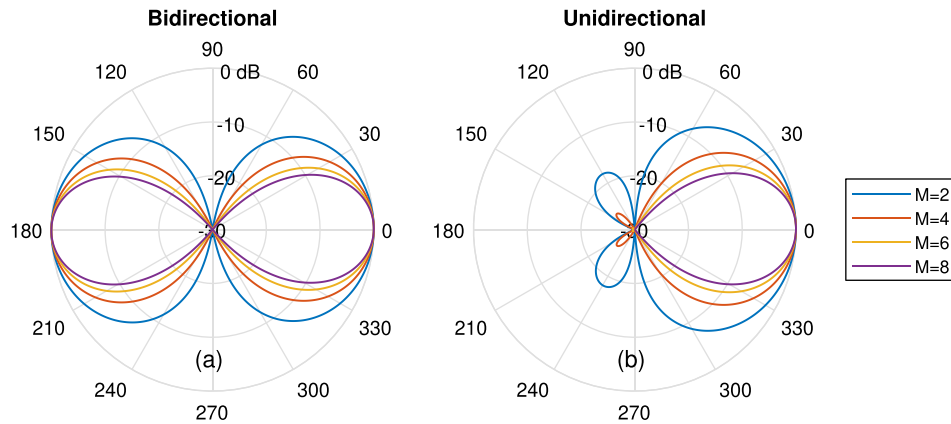


Fig. 2. (Color online) Simulated array response for (a) bidirectional [Eq. (9)] and (b) unidirectional [Eq. (10)] sensors using two microphones and the phase-gradient method, for different orders, M .

of two. This is done by further modifying the directional pressure expression, combining even and odd powers of the directivity factor from Eq. (9). Since odd powers of the directivity factor have a negative response in the back of the array, the array response in that direction nearly cancels when combined with an even power. The unidirectional pressure can be expressed as

$$p_{x,\text{uni}} = \frac{1}{2} \left[\frac{1}{k^M} \left(\frac{\partial \phi}{\partial x} \right)^M + \frac{1}{k^{M-1}} \left(\frac{\partial \phi}{\partial x} \right)^{M-1} \right] P e^{-j\phi}. \quad (10)$$

The resulting unidirectional array response is shown in Fig. 2(b) for several values of M , showing a tighter beam width and suppressed lobes in the back for higher orders.

A final modification allows for computational steering of the array response. With a two-dimensional array, two components of the phase gradient can be estimated. Using both components, the direction of sensitivity is not constrained, and the beam can be steered computationally to an arbitrary angle θ_0 . For a unidirectional sensor,

$$p_{x,\text{uni}} = \frac{1}{2} \left[\frac{1}{k^M} \left(\cos \theta_0 \frac{\partial \phi}{\partial x} + \sin \theta_0 \frac{\partial \phi}{\partial y} \right)^M + \frac{1}{k^{M-1}} \left(\cos \theta_0 \frac{\partial \phi}{\partial x} + \sin \theta_0 \frac{\partial \phi}{\partial y} \right)^{M-1} \right] P e^{-j\phi}, \quad (11)$$

where θ_0 is the angle of maximum sensitivity defined from the x -axis on the x - y plane.

Using these modifications, an array response $\cos^M \theta$ can be created using two microphones. With a two-dimensional array (three or more microphones), the array axis and primary response can be steered to an arbitrary direction, θ_0 . Further manipulation of the directivity factor can lead to additional array responses, suited for a variety of purposes.

3. Experiment

To validate the phase gradient formulation of directional pressure, and to compare the array response with those of other methods, an experiment was performed in an anechoic chamber. A microphone array was attached to a turntable, composed of two perpendicular microphone pairs, each with a separation, $d = 10$ cm (4 in.). The microphones were 1.27 cm (1/2 in.) free-field, condenser microphones, and each pair was phase-matched. One pair acted as a broadside array for time-domain, additive beamforming, and the other pair was used for the pressure-gradient and phase-gradient methods, sensing along the array axis. To map the array response of each two-microphone method, the array was rotated in increments of 5° relative to a fixed loudspeaker 2.1 m (7 ft) away producing white noise. The measurement schematic and array response for several two-microphone processing methods at three frequencies are shown in the top row of Fig. 3.

To compare the methods' ability to resolve a single source, beamforming, traditional gradient sensing, and phase-gradient sensing are compared for the single loudspeaker experiment. While the first two methods have erroneous sidelobes at higher frequencies (e.g., $kd = 2\pi$), the phase-gradient estimate of the directional pressure in Eq. (7) does not; the phase-gradient method shows a successful $\cos^2 \theta$ array response

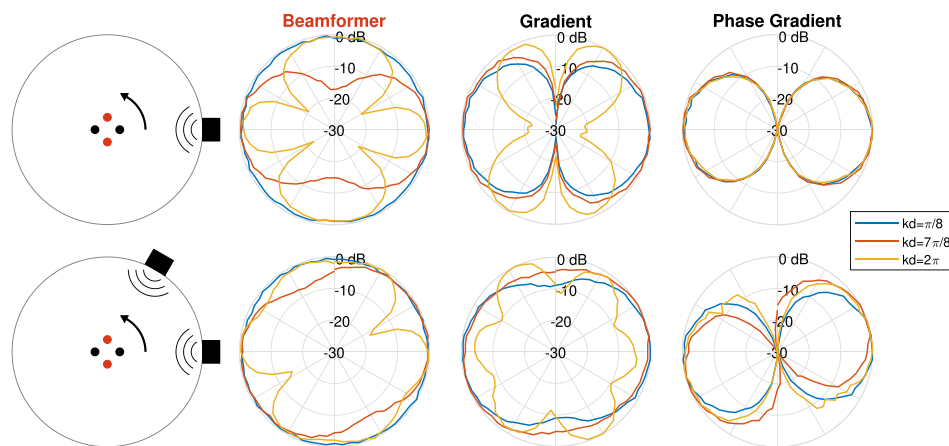


Fig. 3. (Color online) Top: Measured, two-microphone array response using a single loudspeaker at $kd = \pi/8$ (far below spatial Nyquist), $7\pi/8$ (near spatial Nyquist), and 2π (far above spatial Nyquist) using different processing methods: beamforming, traditional gradient sensing, and phase-gradient sensing with phase unwrapping. The gradient and phase gradient sensors were oriented such that at $\theta = 0^\circ$ the microphones (two horizontal dots) were in line with the source, whereas the beamformer requires the source be broadside the microphones (two vertical dots). The microphone separation, d , and source distance in the schematic is not to scale. Bottom: Same for two loudspeakers separated by 60° .

up to the spatial Nyquist frequency ($kd = \pi$) and beyond since the phase gradients can be properly unwrapped. As opposed to the other methods, this phase-gradient method yields consistent results over the entire frequency range where the microphones are receiving sufficiently coherent signals.

A beamformer involves time delays to steer the array,⁹ although in the broadside case investigated here the time delays are zero and the signals are simply added. The broadside beamformer responds nearly omnidirectionally at low frequencies. At high frequencies the pattern becomes more directional, although grating lobes appear above the spatial Nyquist frequency of $kd = \pi$. Additional microphones make beamforming more effective at high frequencies, but the response still varies with frequency, and is nearly omnidirectional at low frequencies (small kd).

A traditional gradient sensor adds pressure signals together multiplied by finite-difference coefficients. In this two-microphone case, one microphone signal is subtracted from the other. This produces a $\cos\theta$ response for low frequencies.¹ However, at frequencies approaching and above the spatial Nyquist frequency ($kd = \pi$), finite-difference errors cause changes in the array response.

To test the methods' behavior in the presence of multiple sources, the experiment was repeated with two incoherent loudspeakers spaced 60° apart, and the results are shown in the bottom row of Fig. 3. None of the two-microphone methods resolve the individual sources. However, the peak response of the phase-gradient method is aimed between the two sources with a well-defined $\cos^2\theta$ pattern, clearly indicating the direction of the group of sources. The response angle at each frequency depends on the relative source amplitudes. The response of the beamformer and traditional gradient sensor have no strong peaks or nulls, resulting in an inconclusive estimate of the location of the group of sources.

In addition to the results above, the array response of the phase-gradient method can be increased by raising the power on the directivity factor, as in Eq. (9). Higher-order estimates calculated from the single-loudspeaker experiment are shown in Fig. 4(a), which match the theoretical patterns shown in Fig. 2(a). Noise in the transfer function phase causes the directivity factor to be slightly higher than 1 when pointed at the source, a small error that is magnified by raising the directivity factor to higher orders. However, the source can still be clearly located even at $M = 8$. Figure 4(b) shows the experimental response of a unidirectional sensor of various orders [Eq. (10)], which can be compared with the theoretical response in Fig. 2(b). The response of the two-dimensional, four-microphone array is displayed in Fig. 4(c) and obtained by computationally steering the unidirectional sensor in Eq. (11) without rotating the array.

4. Conclusion

The phase-gradient method for directional pressure sensing explained in this letter avoids high-frequency, finite-difference error present in other methods through use of the phase gradient, similar to intensity estimation using the PAGE method. This approach allows for the creation of a two-microphone, frequency-domain array

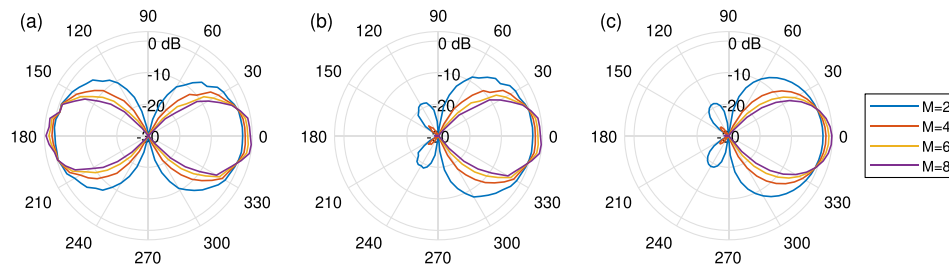


Fig. 4. (Color online) Measured, single-loudspeaker array response for phase-gradient method of order $M = 2, 4, 6,$ and 8 for (a) a two-microphone bidirectional sensor, (b) a two-microphone unidirectional sensor obtained from rotating the array, and (c) a computationally steered two-dimensional, unidirectional sensor, using a single measurement with the loudspeaker at 60° from the x -axis of the 4-microphone array. All data shown are for 200 Hz, which in this case is $kd = 0.37$.

response with an arbitrary directivity order that is accurate up to the spatial Nyquist frequency. For broadband sources and with proper unwrapping, accuracy can be extended up to the limit of inter-microphone coherence.

Conventional gradient-based sensors have the advantage of returning signals in the time domain, allowing for the creation of live filtering such as in a cardioid microphone. However, the array responses of these microphones break down at higher frequencies due to finite-difference errors. Some finite-difference error is avoided by using particle velocity sensors, as done by de Bree and Wind.⁵ However, these sensors can be sensitive to wind noise, complicating outdoor measurements.¹⁹ The phase gradient sensor introduced in this letter allows for accurate estimation at higher frequencies than traditional methods. With proper phase unwrapping, the microphone spacing can be increased as needed to reduce low-frequency error caused by microphone phase mismatch, without losing high-frequency accuracy.

An additive beamformer avoids the finite-difference errors present in gradient microphones; however, the array response changes with frequency. At low frequencies, the response is nearly omnidirectional, whereas at high frequencies the beam is much narrower but grating lobes appear. Beamforming can be used as a time-domain filter, but for use with intensity probes, the dimensions are too small and the microphone count is too low for the beamforming to be effective over most frequencies of interest. These comparisons indicate that phase gradient-based directional sensing is more effective for highly directional frequency-domain pressure sensing using a small number of microphones.

A primary drawback of the phase-gradient method for directional pressure is its limitation to the frequency domain. However, the possibility exists to use the frequency-dependent phase gradient to inform a time-domain filter for stationary systems. By using the phase gradient, the average direction of incoming sound at each frequency could be determined, which could then be used to filter the signal in the time domain. This filtering could either be done in blocks for recorded data or using an adaptive filter in real-time. Source discrimination would be possible up to the spatial Nyquist frequency. The robustness of this approach has yet to be determined.

Acknowledgments

This work was supported by National Science Foundation Grant No. 1538550, “Developing new methods for obtaining energy-based acoustic quantities.”

References and links

- ¹H. F. Olson, “Gradient Microphones,” *J. Acoust. Soc. Am.* **17**, 192–198 (1946).
- ²B. A. Cray, V. M. Evora, and A. H. Nuttall, “Highly directional acoustic receivers,” *J. Acoust. Soc. Am.* **113**, 1526–1532 (2003).
- ³E. De Sena, H. Hacihabiboglu, and Z. Cvetkovic, “On the design and implementation of higher order differential microphones,” *IEEE Trans. Audio Speech Lang. Process.* **20**, 162–174 (2012).
- ⁴K. J. Bastyr, G. C. Lauchle, and J. A. McConnell, “Development of a velocity gradient underwater acoustic intensity sensor,” *J. Acoust. Soc. Am.* **106**, 3178–3188 (1999).
- ⁵H. E. de Bree and J. Wind, “A particle velocity gradient beam forming system,” *J. Acoust. Soc. Am.* **127**, 1820 (2010).
- ⁶S. Yu, D. F. Comesaña, G. C. Pousa, Y. Yang, and L. Xu, “Unidirectional acoustic probe based on the particle velocity gradient,” *J. Acoust. Soc. Am.* **139**, EL179–EL183 (2016).
- ⁷G. M. Sessler and J. E. West, “Second-order gradient unidirectional microphones utilizing an electret transducer,” *J. Acoust. Soc. Am.* **58**, 273–278 (1975).
- ⁸J. C. Chen, K. Yao, and R. E. Hudson, “Source localization and beamforming,” *IEEE Signal Proc. Mag.* **19**(2), 30–39 (2002).

- ⁹B. D. Van Veen and K. M. Buckley, "Beamforming: A versatile approach to spatial filtering," *IEEE ASSP Mag.* **5**, 4–24 (1988).
- ¹⁰A. Nehorai and E. Paldi, "Acoustic vector-sensor array processing," *IEEE Trans. Signal Process.* **42**, 2481–2491 (1994).
- ¹¹D. J. Schmidlin, "Directionality of generalized acoustic sensors of arbitrary order," *J. Acoust. Soc. Am.* **121**, 3569–3578 (2007).
- ¹²M. E. Lockwood and D. L. Jones, "Beamformer performance with acoustic vector sensors in air," *J. Acoust. Soc. Am.* **119**, 608–619 (2006).
- ¹³Y. Song and K. T. Wong, "Azimuth-elevation direction finding using a microphone and three orthogonal velocity sensors as a non-collocated subarray," *J. Acoust. Soc. Am.* **133**, 1987–1995 (2013).
- ¹⁴E. Gorman, S. Bunkley, J. E. Ball, and A. Netchaev, "Direction of arrival estimation for conformal arrays on real-world impulsive acoustic signals," *Proc. Mtgs. Acoust.* **31**, 055003 (2018).
- ¹⁵D. C. Thomas, B. Y. Christensen, and K. L. Gee, "Phase and amplitude gradient method for the estimation of acoustic vector quantities," *J. Acoust. Soc. Am.* **137**, 3366–3376 (2015).
- ¹⁶M. R. Cook, K. L. Gee, S. D. Sommerfeldt, and T. B. Neilsen, "Coherence-based phase unwrapping for broadband acoustic signals," *Proc. Mtgs. Acoust.* **30**, 055005 (2017).
- ¹⁷K. L. Gee, T. B. Neilsen, S. D. Sommerfeldt, M. Akamine, and K. Okamoto, "Experimental validation of acoustic intensity bandwidth extension by phase unwrapping," *J. Acoust. Soc. Am.* **141**, EL357–EL362 (2017).
- ¹⁸E. B. Whiting, J. S. Lawrence, K. L. Gee, T. B. Neilsen, and S. D. Sommerfeldt, "Bias error analysis for phase and amplitude gradient estimation of acoustic intensity and specific acoustic impedance," *J. Acoust. Soc. Am.* **142**, 2208–2218 (2017).
- ¹⁹W. F. Druyvesteyn and H. E. De Bree, "A novel sound intensity probe comparison with the pair of pressure microphones intensity probe," *J. Audio Eng. Soc.* **48**, 49–56 (2000).